

# Antisense Suppression of the Small Chloroplast Protein CP12 in Tobacco Alters Carbon Partitioning and Severely Restricts Growth<sup>1[W]</sup>

Thomas P. Howard<sup>2\*</sup>, Michael J. Fryer, Prashant Singh<sup>3</sup>, Metodi Metodiev, Anna Lytovchenko, Toshihiro Obata, Alisdair R. Fernie, Nicholas J. Kruger, W. Paul Quick<sup>4</sup>, Julie C. Lloyd, and Christine A. Raines

Department of Biological Sciences, University of Essex, Colchester CO4 3SQ, United Kingdom (T.P.H., M.J.F., P.S., M.M., J.C.L., C.A.R.); Department of Lothar Willmitzer, Max-Planck-Institut für Molekulare Pflanzenphysiologie, 14476 Potsdam-Golm, Germany (A.L., T.O., A.R.F.); Department of Plant Sciences, University of Oxford, Oxford OX1 3RB, United Kingdom (N.J.K.); and Department of Animal and Plant Sciences, University of Sheffield, S10 2TN Sheffield, United Kingdom (W.P.Q.)

The thioredoxin-regulated chloroplast protein CP12 forms a multienzyme complex with the Calvin-Benson cycle enzymes phosphoribulokinase (PRK) and glyceraldehyde-3-phosphate dehydrogenase (GAPDH). PRK and GAPDH are inactivated when present in this complex, a process shown *in vitro* to be dependent upon oxidized CP12. The importance of CP12 *in vivo* in higher plants, however, has not been investigated. Here, antisense suppression of CP12 in tobacco (*Nicotiana tabacum*) was observed to impact on NAD-induced PRK and GAPDH complex formation but had little effect on enzyme activity. Additionally, only minor changes in photosynthetic carbon fixation were observed. Despite this, antisense plants displayed changes in growth rates and morphology, including dwarfism and reduced apical dominance. The hypothesis that CP12 is essential to separate oxidative pentose phosphate pathway activity from Calvin-Benson cycle activity, as proposed in cyanobacteria, was tested. No evidence was found to support this role in tobacco. Evidence was seen, however, for a restriction to malate valve capacity, with decreases in NADP-malate dehydrogenase activity (but not protein levels) and pyridine nucleotide content. Antisense repression of CP12 also led to significant changes in carbon partitioning, with increased carbon allocation to the cell wall and the organic acids malate and fumarate and decreased allocation to starch and soluble carbohydrates. Severe decreases were also seen in 2-oxoglutarate content, a key indicator of cellular carbon sufficiency. The data presented here indicate that in tobacco, CP12 has a role in redox-mediated regulation of carbon partitioning from the chloroplast and provides strong *in vivo* evidence that CP12 is required for normal growth and development in plants.

The Calvin-Benson cycle, the primary pathway for carbon fixation, is dependent on the energy (ATP) and reducing power (NADPH) supplied from photosynthetic electron transport to capture atmospheric CO<sub>2</sub>. The supply of ATP and NADPH within the chloroplast, however, can fluctuate in response to variations in light intensity. Therefore, the Calvin-Benson cycle is situated at a critical juncture between environmental

input and biosynthetic output. As a result, the activities of the enzymes of the Calvin-Benson cycle are sensitive to changes in pH, metabolite and Mg<sup>2+</sup> concentrations, and redox state (mediated via the ferredoxin/thioredoxin system; Scheibe, 1991; Geiger and Servaites, 1994). Such mechanisms allow the modulation of enzyme activities during the day and complete suppression at night.

Regulation has also been proposed to occur through the formation of a multiprotein complex between two of the thioredoxin-regulated enzymes, phosphoribulokinase (PRK; EC 2.7.1.19) and glyceraldehyde-3-phosphate dehydrogenase (GAPDH; EC 1.2.1.13), mediated by the small chloroplast protein CP12 (Wedel et al., 1997; Wedel and Soll, 1998; Graciet et al., 2003). Enzyme activity is low during protein aggregation, while dissociation of the complex results in an increase in PRK and GAPDH activity. This complex has been shown to be present in several higher plant species (Wedel et al., 1997; Wedel and Soll, 1998; Scheibe et al., 2002; Howard et al., 2011), in algal species (Avilan et al., 1997; Boggetto et al., 2007; Oesterhelt et al., 2007), and in a cyanobacterium (Tamoi et al., 2005). Furthermore, dissociation and aggregation of this complex in

<sup>1</sup> This work was supported by the Biotechnology and Biological Sciences Research Council (grant nos. P19403 and P19404) and by a University of Essex research start-up grant.

<sup>2</sup> Present address: Biosciences, College of Life and Environmental Sciences, University of Exeter, Exeter EX4 4QD, UK.

<sup>3</sup> Present address: Department of Life Science and Institute of Plant Biology, National Taiwan University, Taipei 106, Taiwan.

<sup>4</sup> Present address: International Rice Research Institute, Los Banos, Laguna 4031, Philippines.

\* Corresponding author; e-mail t.p.howard@exeter.ac.uk.

The author responsible for distribution of materials integral to the findings presented in this article in accordance with the policy described in the Instructions for Authors ([www.plantphysiol.org](http://www.plantphysiol.org)) is: Christine A. Raines ([rainc@essex.ac.uk](mailto:rainc@essex.ac.uk)).

<sup>[W]</sup> The online version of this article contains Web-only data.

[www.plantphysiol.org/cgi/doi/10.1104/pp.111.183806](http://www.plantphysiol.org/cgi/doi/10.1104/pp.111.183806)

pea (*Pisum sativum*) leaves are rapid and respond to light quantity (Howard et al., 2008). Support for the importance of CP12 in mediating the formation of this complex has come from *in vitro* experiments utilizing recombinant expressed proteins or partially purified components. These data have demonstrated that complex formation is dependent upon the presence of oxidized CP12 (Scheibe et al., 2002; Marri et al., 2005), and recent evidence suggests that this is mediated by changes in the redox state of thioredoxin *f* (Howard et al., 2008; Marri et al., 2009).

While the evidence for the existence of the PRK/GAPDH/CP12 complex and the significance of CP12 in mediating complex formation is strong, the importance of CP12 in regulating PRK and GAPDH activities *in vivo* has never been genetically tested. Furthermore, the importance of CP12 in determining *in vivo* photosynthetic capacity has not been addressed. CP12 is known to be necessary to cyanobacterial metabolism, as demonstrated by the fact that the growth of a cyanobacterial CP12 insertional mutant was significantly impaired when grown in light/dark cycles (Tamoi et al., 2005). Analysis of ribulose 5-phosphate levels suggested that formation of the PRK/GAPDH/CP12 complex was essential to separate the activities of the Calvin-Benson cycle from the oxidative pentose phosphate pathway (OPPP). The authors, however, did not report the impact of a loss of CP12 on enzyme activities or on photosynthetic capacity. Furthermore, higher plants differ from cyanobacteria in that not only are some Calvin-Benson cycle enzymes reductively activated in the light but, also, plastidic Glc-6-P dehydrogenase (G6PDH; EC 1.1.1.49), the first enzyme of the OPPP, is reductively inactivated (Wenderoth et al., 1997; Kruger and von Schaewen, 2003; Née et al., 2009). Such a mechanism could be sufficient to prevent futile cycling between the Calvin-Benson cycle and the OPPP. Moreover, recent evidence has shown that there is heterogeneity in PRK and GAPDH regulation by redox changes and by CP12 in algal species (Maberly et al., 2010) and in PRK and GAPDH protein complex profiles in higher plant species (Howard et al., 2011). These reports indicate that the importance of CP12 and of protein aggregation to the regulation of metabolism is likely to vary between species.

The aim of the work presented here was to investigate the importance of CP12 to PRK and GAPDH activity and to Calvin-Benson cycle regulation *in vivo*. To achieve this, antisense CP12 constructs were expressed in tobacco (*Nicotiana tabacum*) with the aim of reducing the amount of CP12 protein. Following confirmation of a repression of CP12 protein levels, we sought to identify the impact on PRK and GAPDH aggregation and enzyme activities as well as on photosynthetic carbon assimilation. We were also able to use these lines to test the hypothesis that CP12 is necessary for the separation of Calvin-Benson cycle and OPPP activities. The data generated from these plants provides evidence that CP12 is an integral component in determining carbon partitioning and that reductions of

CP12 content perturb carbon/nitrogen homeostasis in tobacco leaves.

## RESULTS

### Antisense Repression of CP12 in Tobacco

An antisense gene construct was prepared by inserting a full-length tobacco CP12-A (Pohlmeyer et al., 1996) cDNA fragment downstream of the cauliflower mosaic virus 35S promoter in the vector pBin19. The construct was transferred into tobacco using *Agrobacterium tumefaciens*-mediated leaf-disc transformation, and more than 20 kanamycin-resistant primary transformants were recovered. The resulting T1 progeny were used to generate the T2 and T3 generations analyzed here. PCR analysis confirmed that the transgene was present in the chromosomal DNA (Supplemental Fig. S1). Estimation of CP12 protein content using immunoblot techniques was problematic when used against a complex mixture of proteins. In order to circumvent this, we used the AQUA strategy (Gerber et al., 2003) to quantify a CP12 peptide fragment by comparison with a synthetic stable isotope-labeled peptide as internal standard (see "Materials and Methods"). Using this technique, it was seen that levels of CP12-A protein decreased in all of the tobacco antisense lines compared with the control (Fig. 1). Four independent lines in which CP12-A protein content was reduced by approximately 60% (AS1), 70% (AS43), and 90% (AS2/1 and AS6) were used for subsequent analysis.

### Plant Growth and Development in Antisense Tobacco Lines

Antisense repression of CP12 in tobacco plants resulted in moderate to severe decreases in growth

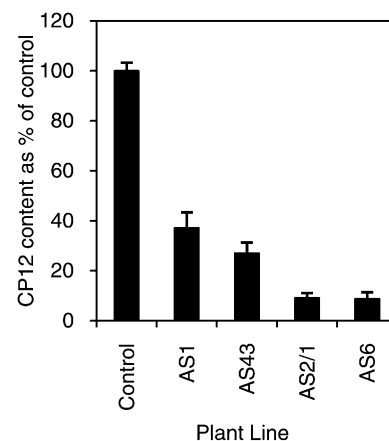


**Figure 1.** Amount of CP12 protein quantified in control and antisense tobacco plants. Values are expressed as percentage of control. Error bars represent SE;  $n = 3$ .

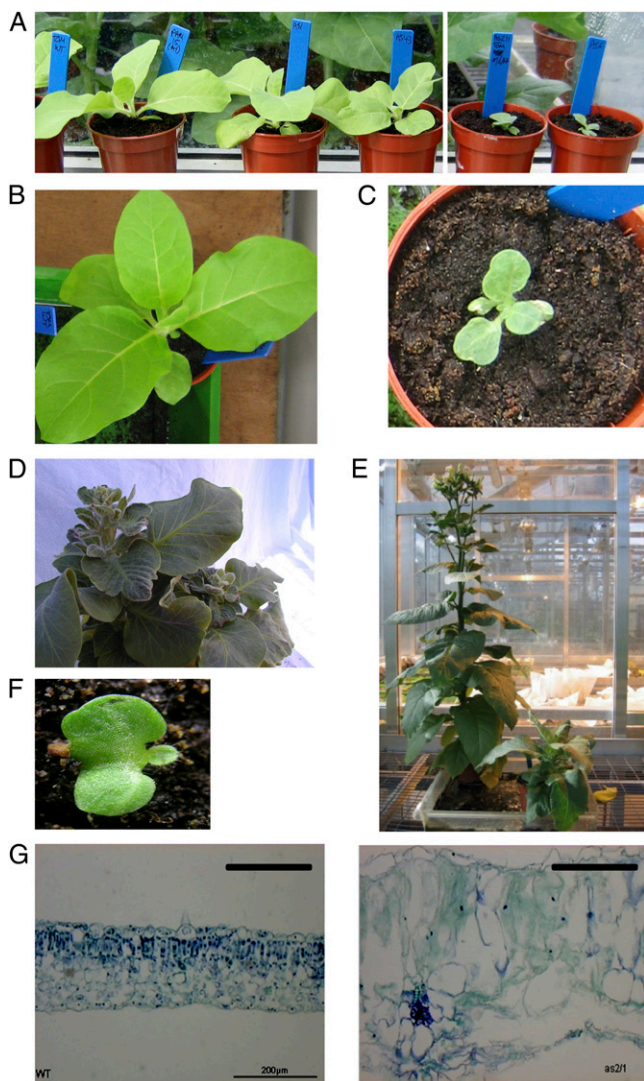


**Figure 2.** Phenotypic changes observed in antisense CP12 tobacco lines. A, Plant growth 6 weeks from sowing in control and antisense tobacco lines (left to right: control, AS1, AS43, AS2/1, and AS6). B and C, Altered leaf morphology in control (B) and AS2/1 (C) tobacco. D, Loss of apical dominance. E and F, Altered leaf morphology at maturity (E) and at the cotyledon stage (F; control [left] and AS2/1 [right]). G, Transverse sections of leaves from control (left) and AS2/1 (right), viewed at the same magnification. Bars = 200  $\mu\text{m}$ .

rate, accompanied by abnormalities in leaf shape and reduced apical dominance (Fig. 2; Supplemental Fig. S2). Lines AS1 and AS43, in which CP12 protein content was reduced by 60% to 70%, displayed less severe alterations than lines AS2/1 and AS6, in which reductions of greater than 90% were observed. Measurements of plant height throughout growth revealed that growth rate was restricted; control plants entered the rapid, exponential phase of growth approximately 40 d after sowing, while in the antisense plants, this occurred approximately 20 d later (Supplemental Fig. S2). The time to flowering was also delayed by more

than 30 d. Leaf morphology was severely affected from the early stages of development to maturity (Fig. 2, B–F), and transverse leaf sections revealed as much as a 3-fold increase in leaf thickness (Fig. 2G). Cell size parameters were determined in one of the tobacco antisense lines displaying morphological changes (AS2/1), and it was found that this increased leaf thickness was accompanied by an increase in cell size rather than number (Table I).

### PRK and GAPDH Complexes and Enzyme Activities

Previously, we have reported that our ability to detect interactions between PRK and GAPDH in darkened leaves of tobacco is dependent on the incubation of stromal samples with  $\text{NAD}^+$  prior to electrophoresis (Howard et al., 2011). This  $\text{NAD}^+$ -induced formation of the complex was evident in stromal proteins of control tobacco as demonstrated (1) by the loss of the dimeric form of PRK and the low- $M_r$  forms of GAPDH (A4 and A2B2) and (2) by the formation of high- $M_r$  aggregates (Fig. 3, A and B). The effect of  $\text{NAD}^+$  on the migration of stromal proteins extracted from the antisense lines was less pronounced. A proportion of dimeric PRK and tetrameric forms of GAPDH were still detectable in lines with the greatest reduction in CP12, while the effect was less pronounced in the line displaying a more modest decrease in CP12 content (AS43). Therefore, the ability of the PRK/GAPDH/CP12 complex to aggregate in response to incubation with  $\text{NAD}^+$  is impaired in the antisense CP12 lines.

Given the proposed role for CP12 in the regulation of PRK and GAPDH activities, the impact of antisense repression of CP12 on enzyme activities was assessed in the three lines with the greatest reductions in CP12. It was observed that the reduction in CP12 content had no effect on the dark deactivation of PRK and GAPDH compared with the control lines (Fig. 3, C and D). We also examined the activity of PRK and GAPDH in illuminated leaves, and again, no significant differences were observed in the activation of PRK and GAPDH between antisense CP12 lines and the control: illumination resulted in the activation of between 86% and 91% of maximal extractable activity. However, there was seen to be a reduction in maximal activity of both PRK and GAPDH in one of the lines (AS6). It is concluded, therefore, that in tobacco, reductions of greater

**Table I.** Leaf cell parameters

Transverse sections of leaves from wild-type plants (control) and CP12 antisense lines (AS2/1) were examined for alterations to leaf cell and chloroplast morphology. Data shown are means and  $\text{SE}$  for 30 mesophyll cells per line.

Plant Line	Cell Area	Cell Length	Cell Width
	$\text{mm}^2$	$\mu\text{m}$	
Control	$7.6 \pm 0.4$	$173 \pm 4.5$	$52.1 \pm 2.1$
AS2/1	$20.2 \pm 1.0$	$259 \pm 11.4$	$100.2 \pm 4.0$

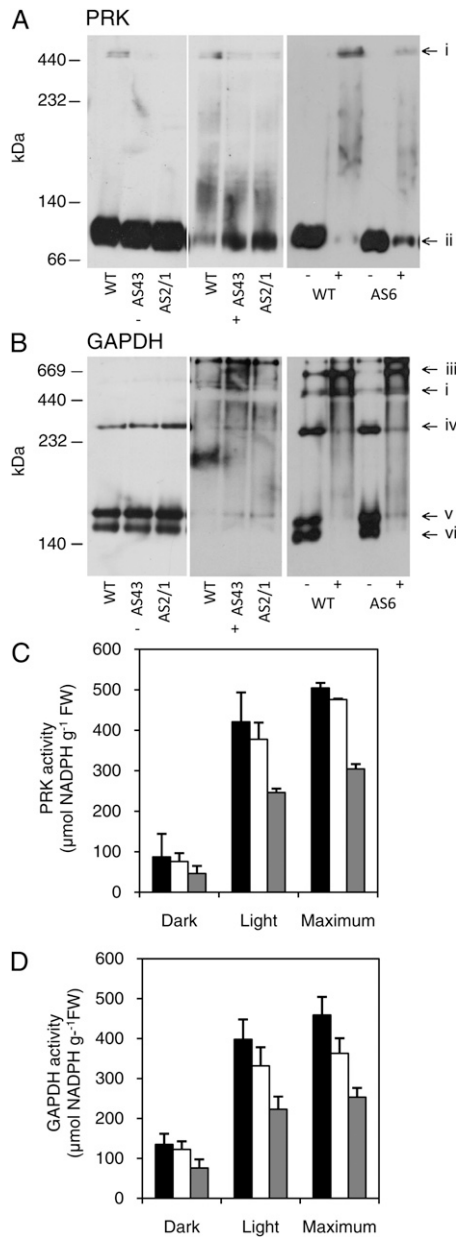


**Figure 3.** PRK and GAPDH aggregation and enzyme activities in antisense CP12 plants. A and B, Immunoblot detection of PRK (A) and GAPDH (B) proteins separated using BN-PAGE. Stromal proteins prepared from darkened leaves were incubated either in the absence (–) or presence (+) of 2.5 mM NAD<sup>+</sup> for 30 min prior to separation. Arrows indicate the locations of PRK and GAPDH protein complexes as identified previously (Howard et al., 2011): i, PRK/GAPDH/CP12; ii, PRK homodimer; iii, A8B8 GAPDH; iv, A4B4 GAPDH; v, A2B2 GAPDH; vi, A4 GAPDH. C and D, PRK (C) and GAPDH (D) activities in leaves from control (black bars), AS2/1 (white bars), and AS6 (gray bars) sampled during darkness, following illumination or following full activation with DTT. Error bars represent SE; *n* = 4. FW, Fresh weight; WT, wild type.

than 90% in CP12 protein content have little effect on the light activation and dark deactivation of PRK and GAPDH.

### Photosynthetic Carbon Assimilation in Antisense CP12 Tobacco

In order to assess the impact of a reduction in CP12 protein on photosynthetic carbon assimilation, assimilation rates under increasing light intensity were determined for control plants and two lines with different reductions in CP12 content (the mild phenotype AS43 and the severe phenotype AS2/1). The results reveal a decrease in light-saturated CO<sub>2</sub> fixation rates of approximately 25% in line AS 2/1 (Fig. 4A). There were no differences between AS43 and control plants. The decrease in light-saturated rates of photosynthesis may be due to several factors, including a limitation of CO<sub>2</sub> at the site of carboxylation, changes to the catalytic activity of Rubisco, and/or changes to the rate of regeneration of ribulose 1,5-bisphosphate. To probe these possibilities, the response of photosynthetic CO<sub>2</sub> assimilation to increasing intercellular CO<sub>2</sub> (net CO<sub>2</sub> assimilation rate [A] versus calculated substomatal CO<sub>2</sub> concentration [C<sub>i</sub>] response curve) was determined (Fig. 4B). These analyses showed that under conditions of saturating light and saturating CO<sub>2</sub>, the rates of photosynthetic carbon assimilation in AS2/1

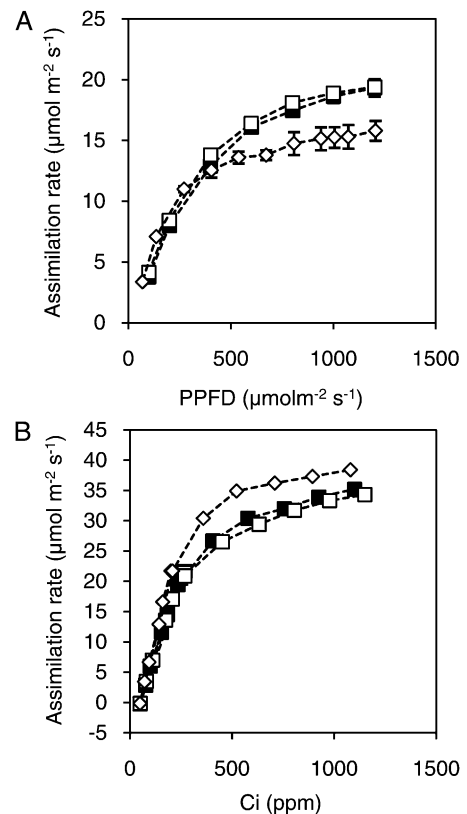


**Figure 4.** Photosynthetic carbon assimilation rates in antisense CP12 plants. A, Carbon assimilation rates at different light intensities. B, Carbon assimilation rates at different CO<sub>2</sub> concentrations. Controls (black squares) and antisense CP12 lines AS43 (white squares) and AS2/1 (white diamonds) are represented. PPF, Photosynthetic photon flux density.

were marginally greater than those of control plants. Given that no changes in stomatal conductance were seen between lines (data not shown), it is likely that the difference between the light response curve and the A/Ci response of line AS2/1 is the result of morphological changes affecting CO<sub>2</sub> diffusion within the leaf.

### Impact of Reduced CP12 Content on the OPPP and the Malate Valve

The redox state of CP12 is mediated by thioredoxin (Marri et al., 2009), and the partially purified PRK/GAPDH/CP12 complex from spinach (*Spinacia oleracea*) has been shown to be influenced by pyridine nucleotides (Wedel et al., 1997; Wedel and Soll, 1998). In addition, data from the CP12 cyanobacterial knock-out mutant suggests that CP12 is necessary to separate the activities of the oxidative and reductive pentose phosphate pathways (Tamoi et al., 2005). To test this hypothesis and to investigate redox homeostasis in the antisense lines, we measured OPPP activity, malate valve capacity, and pyridine nucleotide content.

In higher plants, plastidic G6PDH is the first step in the OPPP, catalyzing the conversion of Glc-6-P to 6-phosphogluconolactone, reducing NADP<sup>+</sup> to NADPH (Kruger and von Schaewen, 2003). As such, it plays a pivotal role in maintaining redox homeostasis. Therefore, the activity of plastidic G6PDH in leaves from control and antisense lines was examined. No differences in total extractable G6PDH activity were detected. Examination of the plastidic isoform (which is dithiothreitol [DTT] sensitive) indicated that there was an increase in plastidial G6PDH activity in the dark compared with the light of approximately 5-fold, consistent with increased OPPP activity in the dark (Fig. 5A). However, no significant differences in plastidial G6PDH activity were detected between plant lines in the light or in the dark. Flux through the OPPP was directly determined in discs from control and antisense transgenic lines (AS43, AS2/1, AS6) harvested at the end of the photoperiod and incubated in the dark in the presence of [1-<sup>14</sup>C]Glc, [2-<sup>14</sup>C]Glc, [3,4-<sup>14</sup>C]Glc, and [6-<sup>14</sup>C]Glc. <sup>14</sup>CO<sub>2</sub> release was determined after a 4-h incubation. The results showed no significant difference between control plants and antisense CP12 lines in the relative yields of CO<sub>2</sub> from different positions within the applied Glc. This suggests that the principal pathways of carbohydrate oxidation in the dark are largely unaffected by differences in CP12 levels. To probe the activity of the OPPP, leaf discs were incubated with either [U-<sup>14</sup>C]Glc or [1-<sup>14</sup>C]gluconate (Table II). Release of <sup>14</sup>CO<sub>2</sub> from the latter occurs specifically during the decarboxylation of 6-phosphogluconate to ribulose 5-phosphate catalyzed by 6-phosphogluconate dehydrogenase and thus provides a direct measure of flux through the oxidative steps of the pentose phosphate pathway (Garlick et al., 2002). The uptake and metabolism of both substrates was significantly greater in the dark than in the light, and the release of <sup>14</sup>CO<sub>2</sub> from [1-<sup>14</sup>C]gluconate relative

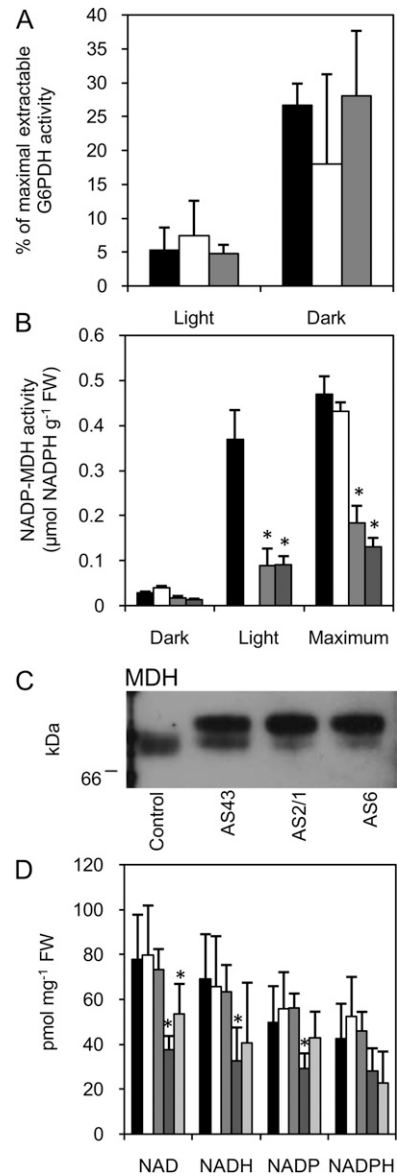


**Figure 5.** Glc-6-P dehydrogenase, NADP-MDH, and pyridine nucleotides in antisense CP12 plants. A, DTT-sensitive (plastidial) G6PDH activity (g<sup>-1</sup> fresh weight [FW]), expressed as a percentage of total extractable G6PDH activity from leaves sampled in the light or dark: control (black bars), AS2/1 (white bars), and AS6 (gray bars). B, NADP-MDH activity in the dark, following illumination or following full activation with DTT: control (black bars), AS1 (white bars; light activation not determined), AS2/1 (gray bars), and AS6 (dark gray bars). C, Immunoblot detection of MDH following separation of stromal proteins prepared from darkened leaves using BN-PAGE. D, Pyridine nucleotide content of illuminated leaves: control (black bars), AS1 (white bars), AS32 (gray bars), AS2/1 (dark gray bars), and AS6 (light gray bars). Error bars represent SE; *n* = 3 to 6 replicates. Asterisks indicate significant differences determined by ANOVA followed by Tukey's test (*P* < 0.05).

to that from [U-<sup>14</sup>C]Glc was preferentially suppressed in the light, consistent with inactivation of the OPPP. However, there was no significant difference between plant lines in the proportion of applied label released

**Table II.** Influence of light on the metabolism of Glc and gluconate by CP12 antisense plants

Leaf discs from control and CP12 antisense lines (AS43, AS2/1, and AS6) harvested after 4 h of illumination were incubated in the presence of [U-<sup>14</sup>C]Glc or [1-<sup>14</sup>C]gluconate in either the light (200 μmol m<sup>-2</sup> s<sup>-1</sup>) or in darkness for 4 h. Metabolized <sup>14</sup>CO<sub>2</sub> was collected. Data are expressed relative to the amount of radioactivity used in the incubation, and each value is the mean ± SE of measurements from four separate leaf discs taken from different plants. The ratios of <sup>14</sup>CO<sub>2</sub> release from [1-<sup>14</sup>C]gluconate/[U-<sup>14</sup>C]Glc are calculated from matched leaf discs taken from the same leaf. This comparison is included to compensate for possible differences in the uptake and metabolism of substrates between the plant lines that may contribute to variations in the amount of <sup>14</sup>CO<sub>2</sub> released from [1-<sup>14</sup>C]gluconate, independent of changes in flux through the OPPP. ANOVA established that the metabolism of both [1-<sup>14</sup>C]gluconate and [U-<sup>14</sup>C]Glc was greater in the dark than in the light (*P* < 0.01), while multivariate ANOVA revealed no significant difference between plant lines in the proportions of <sup>14</sup>CO<sub>2</sub> released from specific substrates incubated under the same conditions.

Plant Line	<sup>14</sup> CO <sub>2</sub> Released from Labeled Substrate				Relative <sup>14</sup> CO <sub>2</sub> Released from [1- <sup>14</sup> C]Gluconate/[U- <sup>14</sup> C]Glc	
	[U- <sup>14</sup> C]Glc		[1- <sup>14</sup> C]Gluconate		Dark	Light
	Dark	Light	Dark	Light		
	% of <sup>14</sup> C applied					
Control	0.35 ± 0.03	0.19 ± 0.03	1.14 ± 0.06	0.06 ± 0.02	3.32 ± 0.27	0.24 ± 0.06
AS43	0.31 ± 0.04	0.19 ± 0.04	1.26 ± 0.08	0.05 ± 0.01	4.36 ± 0.71	0.19 ± 0.05
AS2/1	0.39 ± 0.05	0.25 ± 0.03	1.17 ± 0.08	0.05 ± 0.01	3.13 ± 0.31	0.19 ± 0.04
AS6	0.34 ± 0.05	0.29 ± 0.03	1.19 ± 0.08	0.04 ± 0.01	3.69 ± 0.68	0.15 ± 0.07

as <sup>14</sup>CO<sub>2</sub>. Taken together, these results suggest that CP12 is not essential for regulating flux through the OPPP, nor does it limit the entry of carbon into this pathway in leaves of tobacco in the light.

A second enzyme with a pivotal role in maintaining redox homeostasis in higher plants is NADP-dependent malate dehydrogenase (MDH; EC 1.1.1.82; Backhausen et al., 1994, 1998; Scheibe, 2004). In all lines, it was seen that NADP-MDH activity was suppressed during the dark and activated during the light (Fig. 5B). Activation in the antisense lines, however, was significantly less than in control plants; reductions in the total extractable NADP-MDH activity were also observed. These changes occurred without a reduction in the amount of MDH protein, as estimated by immunoblot detection (Supplemental Fig. S3). Analysis of the migration of native MDH protein from leaf extracts of wild-type and CP12 antisense plants using blue native (BN)-PAGE demonstrated a shift in the mobility of MDH in the antisense lines compared with the wild-type plants, consistent with the reductions in CP12 content (Fig. 5C). From these observations, we conclude that the CP12 antisense lines demonstrate a reduced malate valve capacity. We examined redox homeostasis by examining the pyridine nucleotide content in these plants. NAD<sup>+</sup> was significantly decreased in AS2/1 and AS6, with reductions of between 30% and 50% detected (Fig. 5D). Amounts of NADH and NADPH were also significantly smaller. The ratios of reduced to oxidized forms of each of the pyridine nucleotides were unaltered.

#### Impact of Reductions in CP12 Content on Leaf Carbon/Nitrogen Metabolism

The effects of reduction in CP12 content on leaf metabolism were determined. Carbon partitioning was determined by supplying [U-<sup>14</sup>C]Glc to isolated, illuminated leaf discs. Interestingly, the amount of [<sup>14</sup>C]Glc metabolized by the antisense lines exceeded

that of the control (Supplemental Fig. S4), and there was an increase in partitioning toward the insoluble fraction in the antisense lines compared with the control (Fig. 6A). Within the insoluble fraction, this increase in partitioning was directed specifically toward cell wall and insoluble protein biosynthesis rather than starch biosynthesis (Fig. 6B). Reductions in leaf starch content of approximately 50% in lines AS2/1 and AS6 were confirmed by enzymatic assay (Supplemental Fig. S5). Within the soluble fraction, there was a decrease in partitioning of carbon to soluble sugars and concomitant increases to both the amine and organic acid fractions (Fig. 6C).

The impact of this altered partitioning on metabolite pool sizes was examined in illuminated leaves of the transgenic lines. The results confirm the partitioning data and indicate that the decrease in CP12 led to a significant reduction in soluble carbohydrate pool sizes (Fig. 7A). Most notably, Suc was reduced between 40% and 80% in all lines, including lines AS1 and AS43. Reductions in the levels of Glc, maltose, and trehalose were also seen, although Fru content was largely unaffected. An imbalance of tricarboxylic acid cycle intermediates was also seen: 2-oxoglutarate (2OG) and isocitrate levels were decreased in AS2/1 and AS6, citrate and succinate levels were largely unchanged, while fumarate and malate contents both increased by approximately 50% (Fig. 7B). There were large reductions in several amino acids, including Phe, Trp and Tyr, which are primary products of the shikimate pathway. Shikimate itself was also reduced by more than 50% in the most severely affected lines. These metabolites are of significance as they provide the substrates for lignin biosynthesis. The amounts of the branched chain amino acids Ile and Val were also reduced. By contrast, an increase in the polyamine content was evident in the CP12 antisense lines, in particular the diamine putrescine (Fig. 7D). Pro (which competes with putrescine biosynthesis for Glu) was almost completely absent in the antisense CP12 lines

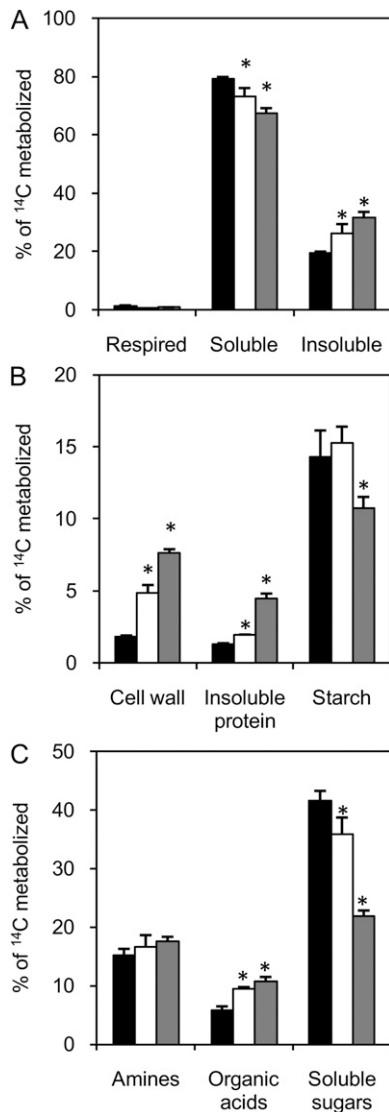


**Figure 6.** Metabolism of [U- $^{14}\text{C}$ ]Glc in illuminated leaves. Control (black bars) and antisense CP12 lines AS2/1 (white bars) and AS6 (gray bars) are represented. A, Partitioning between respiration, soluble, and insoluble fractions. B, Partitioning within the insoluble fraction. C, Partitioning within the soluble fraction. Error bars represent SE;  $n = 3$ . Asterisks indicate significant differences determined by ANOVA followed by Tukey's test ( $P < 0.05$ ).

AS2/1 and AS6. The level of Arg, which is also synthesized from Glu, was also significantly reduced. Taken together, the carbon partitioning and metabolite data indicate that the balance of central carbon and amino acid metabolism is significantly altered in the leaves of plants with decreased CP12 content.

## DISCUSSION

There is strong evidence from partially purified and recombinant protein studies of a central role for CP12 in the formation of a multiprotein complex involving

the enzymes PRK and GAPDH (Wedel et al., 1997; Wedel and Soll, 1998; Scheibe et al., 2002; Graciet et al., 2003; Marri et al., 2008). Complex association/dissociation is rapid and is mediated by changes in the redox state of thioredoxin *f* (Howard et al., 2008; Marri et al., 2009). Taken together, these data suggest a model in which CP12 is an important mediator of PRK and GAPDH activity and that formation/dissociation of this complex exerts control over the rates of carbon assimilation by the Calvin-Benson cycle. In this study, we have taken a transgenic approach to determine the importance of CP12 to the control of PRK and GAPDH activities and to carbon assimilation *in vivo*. The results presented here show that the CP12 antisense tobacco plants displayed a range of aberrant growth phenotypes, including altered leaf morphology, reduced apical dominance, and retarded development. The severity of the changes in development in these plants was unexpected, given the established role for CP12, but they demonstrate that CP12 is crucial for normal plant development.

In the antisense lines, reductions in CP12 protein content of more than 90% had no effect on dark or light activities of PRK and GAPDH. These observations, in conjunction with the inability to detect the high- $M_r$  PRK/GAPDH/CP12 complex in darkened leaves (without incubation in the presence of  $\text{NAD}^+$ ), strongly suggest that, in tobacco leaves, and under the conditions tested in this work, the importance of PRK/GAPDH/CP12 aggregation to the regulation of the Calvin-Benson cycle may be minimal. This conclusion is supported by the observation that even reductions of greater than 90% in CP12 protein content result in minimal effects on  $\text{CO}_2$  fixation rates, effects that could be overcome by increasing substrate ( $\text{CO}_2$ ) concentration. While this may run counter to the original model of CP12 action, recent reports have indicated that differences exist in the regulation of PRK and GAPDH by CP12 across different algal species and in higher plant species (Maberly et al., 2010; Howard et al., 2011). Our conclusion, therefore, does not negate a role for the PRK/GAPDH/CP12 complex in other species but raises a question regarding the ubiquity of such regulatory mechanisms across different species.

In contrast to the small changes in photosynthetic capacity, large shifts in the carbon allocation pattern and metabolite content were evident. The reductions in the levels of starch, Suc, maltose, and trehalose were much greater than expected from the small changes in photosynthetic carbon assimilation observed (Stitt and Schulze, 1994; Raines, 2003). Conversely, significant increases in leaf malate and fumarate content were seen. Fumarate and malate are in close equilibrium and can act as a significant carbon sink in leaves, particularly when starch biosynthesis is impaired (Chia et al., 2000). In addition, a substantial shift in carbon partitioning from soluble components to cell wall biosynthesis occurred that may contribute to the changes in cell morphology. The impact of altered carbon partitioning can also be seen in the dramatic reductions in

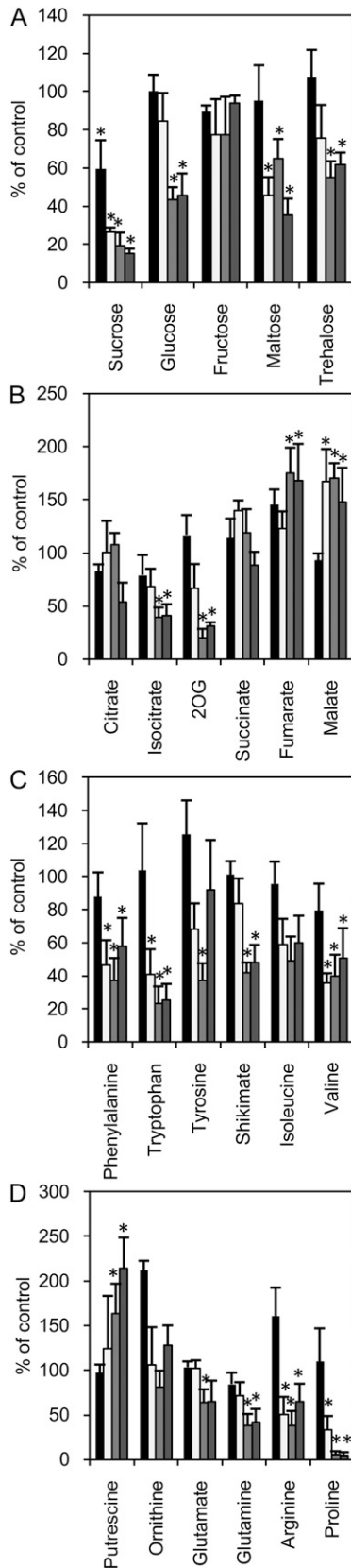


**Figure 7.** Metabolite composition of illuminated leaves of antisense CP12 lines. Antisense lines AS1 (black bars), AS43 (white bars), AS2/1

(gray bars), and AS6 (dark gray bars) are represented. All values are expressed as percentage of control values. A, Soluble carbohydrate content. B, Tricarboxylic acid cycle intermediates. C, Shikimate pathway metabolites and branched amino acids. D, Metabolites related to polyamine metabolism. Error bars represent  $se$ ;  $n = 4$  replicates. Asterisks indicate significant differences determined by ANOVA followed by Tukey's test ( $P < 0.05$ ).

2OG content (between 45% and 80% reductions in the transgenic lines). 2OG is indicative of cellular carbon and nitrogen sufficiency (Lancien et al., 2000; Araújo et al., 2008; Bunik and Fernie, 2009) and is essential for the operation of the GS/GOGAT cycle within the chloroplast. Severe reductions in 2OG would lead to substrate limitation for nitrate reduction (Schneidereit et al., 2006), consistent with the observed decreases in the amounts of many amino acids. 2OG also acts as a regulatory molecule, affecting the activity of cytosolic pyruvate kinase, phosphoenolpyruvate carboxykinase, mitochondrial citrate synthase, and the alternative oxidase (Podestá and Plaxton, 1991; Millar et al., 1993; Wingler et al., 1999; Hodges, 2002). In mammalian and bacterial systems, diverse signaling roles for 2OG have been identified, and there is evidence for the existence of a similar mechanism in plants involving nitrogen status and the PII protein (Hsieh et al., 1998; Smith et al., 2003; Uhrig et al., 2009). Significant decreases in 2OG availability, therefore, are likely to alter mitochondrial, cytosolic, and chloroplastic metabolism and impact on the coordination of carbon-skeleton production and the regulation of cellular redox status via the malate valve.

The redox state of CP12 has been shown to be dependent on thioredoxin (Marri et al., 2009), and there is some evidence for a role for pyridine nucleotides in the aggregation of a partially purified PRK/GAPDH/CP12 complex from spinach (Wedel et al., 1997; Wedel and Soll, 1998). Furthermore, data from a cyanobacterial knockout mutant led to the proposal that CP12 is necessary for the deactivation of PRK in the dark to separate the activities of the OPPP and the reductive pentose phosphate pathway (Tamoi et al., 2005). Given the strong phenotypic and metabolic changes in the antisense plants, we explored the possibility that CP12 may be involved in regulating additional redox-mediated processes in the chloroplast. To explore this, we determined flux through the OPPP, pyridine nucleotide content, and malate valve capacity, estimated through NADP-MDH activity. These data indicated that while OPPP flux was not altered in any of the antisense lines, pyridine nucleotide content and malate valve capacity both decreased. NADP-MDH plays a key role in the stroma, contributing to the maintenance of the redox balance through the reduction of oxaloacetate and the transport of reducing power out of the chloroplast in the form of malate via the 2OG/malate countertransporter (the malate valve; Backhausen et al., 1994; Scheibe, 2004; Scheibe et al., 2005; Schneidereit et al., 2006). In the

(gray bars), and AS6 (dark gray bars) are represented. All values are expressed as percentage of control values. A, Soluble carbohydrate content. B, Tricarboxylic acid cycle intermediates. C, Shikimate pathway metabolites and branched amino acids. D, Metabolites related to polyamine metabolism. Error bars represent  $se$ ;  $n = 4$  replicates. Asterisks indicate significant differences determined by ANOVA followed by Tukey's test ( $P < 0.05$ ).

antisense CP12 lines AS2/1 and AS6, light induction of NADP-MDH was decreased by 50% to 60% and the mobility of the NADP-MDH protein using BN-PAGE was altered. This suggests that the enzyme is present in an inactive conformation in the antisense plants, perhaps trapped in a permanently oxidized state, or subject to other posttranslation modifications that may alter its mobility (e.g. dephosphorylation). However, while it is concluded that a reduction in CP12 protein content has resulted in a decrease in malate valve capacity in the antisense lines, it has not been established whether this is a direct result of the decrease in CP12 content or is in response to decreased pyridine nucleotide content. At this stage, it is not possible to determine if either of these changes are cause or effect; however, it is interesting that CP12 is known to interact with thioredoxin *f*, which in turn is known to antagonistically regulate NADP-MDH and G6PDH and thus redox homeostasis. Changes in levels of 2OG, malate, and NADPH do suggest that, in addition to significant changes in carbon allocation, there is also a change in redox homeostasis. It is also interesting that tobacco lines displaying antisense repression or sense overexpression of pea NADP-MDH demonstrate a significant positive correlation between NADP-MDH activity and growth rates during the maximal growth period (Faske et al., 1997). It has also been shown that a reduced capacity for malate export from the chloroplast through antisense repression of the malate/2OG countertransporter DiT1 in tobacco altered flux to Suc and amino acids and resulted in altered leaf shape and retarded development (Schneidereit et al., 2006). Similarly, loss of the equivalent gene in *Arabidopsis thaliana*; AtpOMT1 results in slow growth and frequently emerging shoots (Kinoshita et al., 2011). These phenotypic changes are similar to those described for the antisense CP12 plants.

The results presented in this paper reveal the importance of the small redox-sensitive chloroplast protein CP12 for normal growth and development in higher plants. As discussed, this may be due in part to the changes observed in malate valve capacity. Given the complexity of the metabolic and developmental phenotype in the antisense plants, however, it is possible that CP12 may have additional functions. Bioinformatic and experimental evidence has shown that CP12 is an intrinsically unstructured protein (Graciet et al., 2003; Gardebien et al., 2006; Marri et al., 2009; Groben et al., 2010). Such proteins can have multiple partners and are frequently considered to be regulatory hubs (Tompa, 2002; Dunker et al., 2005). Therefore, it is possible that CP12 has been coopted into the regulation of other enzymatic partners, and there is already precedence for such an occurrence: CP12 has been shown to interact with plastid aldolase in *Chlamydomonas reinhardtii* (Erales et al., 2008). In addition, transcript analysis of CP12 in *Arabidopsis* has shown that expression is not restricted to photosynthetic tissue, indicating that the role for these proteins is not restricted to the PRK/GAPDH complex (Singh

et al., 2008). Finally, CP12 is a highly conserved protein found in almost all photosynthetic organisms so far examined. CP12 gene sequences from higher plants, mosses, and the green algal group Mesostigmatophyceae are indicative of more disordered proteins than older clades examined (Groben et al., 2010). Such an evolutionary trend toward increased protein disorder suggests that higher plant CP12 may have multiple partners. These reports raise the hypothesis that CP12 function is not restricted to the formation of the PRK and GAPDH complex. While the molecular mechanism of CP12 remains to be resolved, the work presented here provides, to our knowledge, the first *in vivo* evidence supporting this hypothesis and demonstrates that CP12 is essential to maintain metabolic balance in plants.

## MATERIALS AND METHODS

### Chemicals and Reagents

[1-<sup>14</sup>C]Glc (2.00 GBq mmol<sup>-1</sup>), [6-<sup>14</sup>C]Glc (2.07 GBq mmol<sup>-1</sup>), and [U-<sup>14</sup>C]Glc (10.4 GBq mmol<sup>-1</sup>) were purchased from GE Healthcare Life Sciences. [3,4-<sup>14</sup>C]Glc (1.11 GBq mmol<sup>-1</sup>) and [1-<sup>14</sup>C]gluconate (1.85 GBq mmol<sup>-1</sup>) were purchased from American Radiolabeled Chemicals, and [2-<sup>14</sup>C]Glc (1.67 GBq mmol<sup>-1</sup>) was obtained from Perkin-Elmer NEN.

### Plant Growth

Tobacco (*Nicotiana tabacum*) plants were germinated and grown in soil in a controlled-environment greenhouse (25°C–30°C day/20°C night with a 16-h photoperiod, natural light, supplemented with high-pressure sodium light bulbs, giving 600–1,600 μmol m<sup>-2</sup> s<sup>-1</sup> from the pot to the top of the plant). Plants were watered with Hoagland nutrient medium (Arnon and Hoagland, 1940).

### Generation of the Transgenic Plants

A tobacco full-length CP12 cDNA was cloned into the binary vector pAM194 containing the cauliflower mosaic virus 35S promoter and NOS terminator sequences. The recombinant plasmid was introduced into tobacco cv Samsun using *Agrobacterium tumefaciens* LBA4404 via leaf-disc transformation (Horsch et al., 1985). Shoots were regenerated on selective medium containing kanamycin (50 mg L<sup>-1</sup>), and primary transformants (T0) were allowed to self-fertilize.

### Quantification of CP12 Protein

Quantification of CP12 followed the AQUA method described by Gerber et al. (2003), in which synthesized peptides, incorporating stable isotopes, are used as internal standards to mimic native peptides formed by proteolysis. Two leaves from each plant were extracted for each analysis. Proteins were extracted in SDS-PAGE sample buffer and were separated on an 8% SDS-PAGE gel. The protein fraction migrating at the front of the gel was excised and digested in-gel with trypsin. The peptides were extracted, evaporated in a vacuum concentrator, and dissolved in 10 mL of 0.1% aqueous formic acid containing labeled AQUA peptide (LSDLVAESVK) at 100 fmol mL<sup>-1</sup>. The peptide mixtures were injected automatically and analyzed by LTQ Orbitrap Velos in mixed scan mode, where the Orbitrap analyzer scans from 400 to 600 mass-to-charge ratio and the linear ion trap sequentially acquires tandem mass spectrometry spectra on the labeled and native peptides. Both were measured by full scan at a resolution of 30,000 in the Orbitrap analyzer and plotted at a tolerance of 10 ppm around the mass-to-charge ratio of the precursor.

### Anatomical Analysis

Leaves were fixed for 2 h in 0.1 M PIPES buffer containing 3% (v/v) glutaraldehyde and 4% (v/v) paraformaldehyde (pH 7.6). After incubation in

1% (v/v) aqueous osmium tetroxide, tissue was dehydrated and embedded in Spurr resin. Sections of 1  $\mu\text{m}$  thickness were cut on a Cambridge-Huxley microtome and stained for 30 s at 60°C with toluidine blue. Sections were viewed with a Nikon Optiphot microscope, and quantitation of anatomical features used a Lucia image-analysis system (Nikon) linked to the microscope by a TK-128OE JVC CCD camera.

### Protein Extraction and Western Blotting

Chloroplast isolation and BN-PAGE procedures followed the protocols described by Howard et al. (2008, 2011).

### Leaf Material for Enzyme Assays

The most recently fully expanded leaf (leaf 8) was used for analysis. For dark-adapted samples, plants were placed in darkness at the end of a normal photoperiod; leaf discs (1.2 cm diameter) were collected under green safelight after 12 h. For the light-activation investigations, plants were transferred to a growth cabinet at a light intensity of 750  $\mu\text{mol m}^{-2} \text{s}^{-1}$  (24°C and 80% humidity) for 1 h prior to sampling. Leaf discs were frozen in liquid  $\text{N}_2$  immediately after harvesting.

### PRK and GAPDH Activities

Leaf discs were extracted into 1 mL of ice-cold extraction buffer containing 100 mM Tricine (pH 8.0), 10 mM  $\text{MgCl}_2$ , 1 mM EDTA, 15 mM 2-mercaptoethanol, and 0.05% Triton X-100 (v/v) followed by centrifugation at 13,000g for 5 s to remove particulate matter while minimizing light-induced changes in the activation state. The resulting supernatant was assayed immediately. For total extractable activities, the extraction buffer contained 20 mM DTT and the supernatant was incubated on ice for 1 h to achieve full activation, a time period that had no detrimental effect upon enzyme activity (Paul et al., 1995). PRK was assayed by coupling the formation of ADP to the oxidation of NADH monitored at 340 nm and 24°C in reaction mixture containing 50 mM HEPES (pH 7.8), 40 mM KCl, 8 mM  $\text{MgCl}_2$ , 0.25 mM NADH, 2 units  $\text{mL}^{-1}$  pyruvate kinase, 2 units  $\text{mL}^{-1}$  lactate dehydrogenase, 1 mM phosphoenolpyruvate, 1 mM ATP, 0.5 mM ribulose-5-phosphate (and 4 mM DTT for total extractable activities), and the reaction was initiated by the addition of 10  $\mu\text{L}$  of extract in a total reaction volume of 500  $\mu\text{L}$ . NADP-dependent GAPDH activity was assayed in reaction mixture containing 50 mM Tris-HCl (pH 7.8), 10 mM  $\text{MgCl}_2$ , 1 mM EDTA, 2.5 mM ATP, 0.15 mM NADPH or NADH, 5 mM 3-phosphoglyceric acid, 20 units  $\text{mL}^{-1}$  3-phosphoglyceric phosphokinase (and 4 mM DTT for total extractable activity) and initiated by the addition of 10  $\mu\text{L}$  of extract in a total reaction volume of 500  $\mu\text{L}$ .

### G6PDH Activity

Frozen leaf discs were extracted in 1 mL of 100 mM Tris-maleate buffer (pH 8.0) containing 5 mM 2-mercaptoethanol, 0.1 mM  $\text{NADP}^+$ , 1 mM 4-(2-aminoethyl)-benzenesulfonyl fluoride, and 1:100 (v/v) protease inhibitor mix for use with plant extracts and tissues (Sigma-Aldrich). The frozen powdered extract was transferred to a 1.5-mL microfuge tube containing 11 mg of insoluble polyvinylpyrrolidone. The mixture was allowed to thaw, mixed, and centrifuged for 5 min at 4°C and 13,000g. The supernatant was assayed for G6PDH activity in a standard reaction mixture consisting of 2 mM Glc-6-P and 0.2 mM  $\text{NADP}^+$  in nitrogen-sparged 100 mM Tris-maleate (pH 8.0). Cytosolic (DTT-insensitive) isozymes were assayed by diluting an aliquot of the supernatant with 300 mM nitrogen-sparged Tris-maleate buffer (pH 8.0) containing DTT (final concentration, 62.5 mM). For total activity, DTT was omitted. Samples were incubated for 10 min at 24°C prior to addition to the reaction mixture. The reaction was monitored at 340 nm, and plastidic G6PDH activity was determined from the difference between total activity (no DTT) and cytosolic activity (with DTT).

### NADP-MDH Activity

A method modified from that described by Ruuska et al. (2000) was used to determine the activation state of chloroplast NADP-MDH. All solutions were nitrogen sparged prior to use. Frozen leaf discs were extracted in 1 mL of ice-cold buffer containing 50 mM Na-acetate (pH 6.0), 1% (w/v) bovine serum albumin, 4 mM DTT, 0.1% (w/v) Triton X-100, 0.5 mM benzimidazole, 0.5 mM

$\epsilon$ -aminocaproic acid, and 0.5 mM phenylmethylsulfonyl fluoride and centrifuged at 13,000g for 5 min at 4°C. NADP-MDH activity was assayed immediately by the addition of 50  $\mu\text{L}$  of supernatant to a reaction mixture containing 100 mM Tris-HCl (pH 8.0), 1 mM EDTA, 1 mM DTT, and 0.2 mM NADPH. The reaction was initiated by the addition of 2 mM oxaloacetic acid. Loss of NADPH was monitored at 340 nm. In order to assay maximum catalytic activity of reductively activated NADP-MDH, an aliquot of the same supernatant was first incubated in 250 mM Tris-HCl (pH 9.0) containing 125 mM DTT at 24°C for 15 min and then assayed as above. Correction for background activity of NAD-MDH was performed by assaying 10  $\mu\text{L}$  of diluted supernatant in 100 mM Tris-HCl (pH 8.0), 10 mM  $\text{MgCl}_2$ , and 0.2 mM NADH and starting the reaction with 1 mM oxaloacetic acid.

### Gas-Exchange Analysis

Gas-exchange analysis was carried out using a portable gas-exchange system (LI-6400; LI-COR). The baseline was set daily using anhydrous calcium carbonate to remove water and soda lime to remove  $\text{CO}_2$ . A Peltier cooling system maintained leaf temperature at 25°C, and vapor pressure deficit was controlled between 0.7 and 1.4. Leaf photosynthetic  $\text{CO}_2$  uptake rate was determined in response to step changes in quantum flux, provided by an integral light-emitting diode light source. For A/Ci responses, leaves were illuminated using a red-blue light source at 1,200  $\mu\text{mol m}^{-2} \text{s}^{-1}$ . Leaf vapor pressure deficit was maintained between 0.5 and 1.6 kPa. Measurements of photosynthetic carbon assimilation were made starting at 400  $\mu\text{mol mol}^{-1}$   $\text{CO}_2$  surrounding the leaf, decreased stepwise to 50  $\mu\text{mol mol}^{-1}$ , returned to 400  $\mu\text{mol mol}^{-1}$ , and then increased stepwise to 1,600  $\mu\text{mol mol}^{-1}$   $\text{CO}_2$ . Each curve consisted of measurements at a minimum of nine different  $\text{CO}_2$  concentrations.

### Analysis of the Metabolism of $^{14}\text{C}$ -Labeled Substrates by Tobacco Leaves

Plants were grown at 24°C in a 10-h/14-h light/dark cycle with a light level of 200  $\mu\text{mol m}^{-2} \text{s}^{-1}$ . Individual leaf discs (8 mm) were floated on 200  $\mu\text{L}$  of 2 mM sodium bicarbonate, 2 mM [ $^{14}\text{C}$ ]Glc (9.25 MBq  $\text{mmol}^{-1}$ ), or 0.3 mM [ $^{14}\text{C}$ ] gluconate (61.67 MBq  $\text{mmol}^{-1}$ ) and incubated in the light or the dark for 4 h at 22°C or 26°C. The discs were washed, transferred to 80% ethanol, and extracted at 80°C for 40 min. The ethanol-insoluble material was reextracted with 70% ethanol for 40 to 60 min. The ethanol-soluble extracts were combined and adjusted to 1.5 mL with 70% ethanol. Radioactivity was determined in a 0.2-mL aliquot of this fraction. The remainder was evaporated to dryness and suspended in 0.5 mL of water before separation into basic, acidic, and neutral fractions (Kruger et al., 2007).

Ethanol-insoluble material was analyzed by resuspending in 0.2 mL of 0.4 M KOH and incubating for 30 min. Each sample was then neutralized by the addition of 800 mM (100  $\mu\text{L}$ ) acetic acid. Starch was hydrolyzed by combining the sample with 0.54 mL of 0.1 M sodium acetate (pH 5.5) containing 1 unit of amyloglucosidase and 30 units of  $\alpha$ -amylase and incubating at 30°C for 16 h. Subsequently, each sample was centrifuged at 13,000g for 10 min, the supernatant was removed, and the pellet was washed with 1 mL of water. The supernatants were combined, and an aliquot of the sample following digestion was separated by cation-exchange chromatography (Kruger et al., 2007). The resulting aqueous neutral and basic fractions represented starch and protein, respectively. The remaining undigested residue consisting of cell wall material was suspended in 0.2 mL of water prior to the measurement of  $^{14}\text{C}$ .

Metabolized  $^{14}\text{CO}_2$  generated during the incubation was captured in 50  $\mu\text{L}$  of 10% (w/v) KOH in a vial suspended in the sealed incubation vessel (Harrison and Kruger, 2008). Radioactivity was determined in aqueous samples by liquid scintillation counting after combining an appropriate aliquot of each fraction with 4 volumes of Optiphase HiSafe scintillation fluid. Counting efficiency was typically greater than 90%.

### Determination of Pyridine Nucleotides

Extraction of pyridine nucleotide was based on the methods of Hajirezaei et al. (2002) from 25 mg (fresh weight) of leaf material. Standards (0–20 pmol) for each pyridine nucleotide were prepared in the same manner. Assay methods followed Gibon et al. (2002), and the amount of pyridine nucleotides was calculated by comparison with the standard curve.

## Metabolite Profiling

Metabolite analysis was carried out using a gas chromatography-time of flight-mass spectrometry protocol (Lisec et al., 2006). Relative metabolite contents were calculated as described by Roessner et al. (2000) following peak identification using TAGfinder (Luedemann et al., 2008) and spectral libraries housed in the Golm Metabolome Database (Kopka et al., 2005).

## Statistical Analysis

Statistical analysis was performed using Minitab version 11.0 or PASW Statistics 18 (SPSS). Analysis of percentage values was conducted following arcsine [ $\arcsin(y/100)0.5$ ] transformation and on ratios after logarithmic transformation.

## Supplemental Data

The following materials are available in the online version of this article.

**Supplemental Figure S1.** PCR analysis demonstrating the presence of the transgenic construct within the chromosomal DNA.

**Supplemental Figure S2.** Plant height of antisense CP12 lines throughout growth.

**Supplemental Figure S3.** Western-blot analysis of malate dehydrogenase using SDS-PAGE separation.

**Supplemental Figure S4.** Amount of [ $U\text{-}^{14}\text{C}$ ]Glc metabolized by the control and transgenic lines.

**Supplemental Figure S5.** Leaf starch content of antisense lines sampled at the end of the day.

## ACKNOWLEDGMENTS

We thank Drs. P. Davey and T. Lawson (University of Essex, UK) for help with gas-exchange analysis. We also thank Prof. M. Salvucci (Arid-Land Agricultural Research Center, Maricopa, AZ), Dr. N. Wedel (Heinrich-Hecht-Platz, Kiel, Germany), and Prof. Renate Scheibe (University of Osnabrück, Germany) for the PRK, GAPDH, and MDH antibodies, respectively. We are grateful to Dr. E. Kinsman (University of Roehampton, UK) for the data in Figure 2G and Table I.

Received July 25, 2011; accepted August 23, 2011; published August 24, 2011.

## LITERATURE CITED

- Araújo WL, Nunes-Nesi A, Trenkamp S, Bunik VI, Fernie AR (2008) Inhibition of 2-oxoglutarate dehydrogenase in potato tuber suggests the enzyme is limiting for respiration and confirms its importance in nitrogen assimilation. *Plant Physiol* **148**: 1782–1796
- Arnon DI, Hoagland DR (1940) Crop production in artificial culture solutions and in soils with special reference to factors influencing yields and absorption of inorganic nutrients. *Soil Sci* **50**: 463–485
- Avilan L, Gontero B, Lebreton S, Ricard J (1997) Memory and imprinting effects in multienzyme complexes. I. Isolation, dissociation, and reassociation of a phosphoribulokinase-glyceraldehyde-3-phosphate dehydrogenase complex from *Chlamydomonas reinhardtii* chloroplasts. *Eur J Biochem* **246**: 78–84
- Backhausen JE, Emmerlich A, Holtgreve S, Horton P, Nast G, Rogers JJM, Muller-Rober B, Scheibe R (1998) Transgenic potato plants with altered expression levels of chloroplast NADP-malate dehydrogenase: interactions between photosynthetic electron transport and malate metabolism in leaves and in isolated intact chloroplasts. *Planta* **207**: 105–114
- Backhausen JE, Kitzmann C, Scheibe R (1994) Competition between electron acceptors in photosynthesis: regulation of the malate valve during  $\text{CO}_2$  fixation and nitrite reduction. *Photosynth Res* **42**: 75–86
- Boggetto N, Gontero B, Maberly SC (2007) Regulation of phosphoribulokinase and glyceraldehyde 3-phosphate dehydrogenase in a freshwater diatom, *Asterionella formosa*. *J Phycol* **43**: 1227–1235
- Bunik VI, Fernie AR (2009) Metabolic control exerted by the 2-oxoglutarate dehydrogenase reaction: a cross-kingdom comparison of the cross-road between energy production and nitrogen assimilation. *Biochem J* **422**: 405–421
- Chia DW, Yoder TJ, Reiter WD, Gibson SI (2000) Fumaric acid: an overlooked form of fixed carbon in *Arabidopsis* and other plant species. *Planta* **211**: 743–751
- Dunker AK, Cortese MS, Romero P, Iakoucheva LM, Uversky VN (2005) Flexible nets: the roles of intrinsic disorder in protein interaction networks. *FEBS J* **272**: 5129–5148
- Erales J, Avilan L, Lebreton S, Gontero B (2008) Exploring CP12 binding proteins revealed aldolase as a new partner for the phosphoribulokinase/glyceraldehyde 3-phosphate dehydrogenase/CP12 complex: purification and kinetic characterization of this enzyme from *Chlamydomonas reinhardtii*. *FEBS J* **275**: 1248–1259
- Faske M, Backhausen JE, Sendker M, Singer-Bayrle M, Scheibe R, Von Schaewen A (1997) Transgenic tobacco plants expressing pea chloroplast Nmdh cDNA in sense and antisense orientation (effects on NADP-malate dehydrogenase level, stability of transformants, and plant growth). *Plant Physiol* **115**: 705–715
- Gardebien F, Thangudu RR, Gontero B, Offmann B (2006) Construction of a 3D model of CP12, a protein linker. *J Mol Graph Model* **25**: 186–195
- Garlick AP, Moore C, Kruger NJ (2002) Monitoring flux through the oxidative pentose phosphate pathway using [ $1\text{-}^{14}\text{C}$ ]gluconate. *Planta* **216**: 265–272
- Geiger DR, Servaites JC (1994) Diurnal regulation of photosynthetic carbon metabolism in C3 plants. *Annu Rev Plant Physiol Plant Mol Biol* **45**: 235–256
- Gerber SA, Rush J, Stemman O, Kirschner MW, Gygi SP (2003) Absolute quantification of proteins and phosphoproteins from cell lysates by tandem MS. *Proc Natl Acad Sci USA* **100**: 6940–6945
- Gibon Y, Vigeolas H, Tiessen A, Geigenberger P, Stitt M (2002) Sensitive and high throughput metabolite assays for inorganic pyrophosphate, ADPGlc, nucleotide phosphates, and glycolytic intermediates based on a novel enzymic cycling system. *Plant J* **30**: 221–235
- Graciet E, Gans P, Wedel N, Lebreton S, Camadro JM, Gontero B (2003) The small protein CP12: a protein linker for supramolecular complex assembly. *Biochemistry* **42**: 8163–8170
- Groben R, Kaloudas D, Raines CA, Offmann B, Maberly SC, Gontero B (2010) Comparative sequence analysis of CP12, a small protein involved in the formation of a Calvin cycle complex in photosynthetic organisms. *Photosynth Res* **103**: 183–194
- Hajirezaei MR, Peisker M, Tschiersch H, Palatnik JF, Valle EM, Carrillo N, Sonnewald U (2002) Small changes in the activity of chloroplastic NADP(+)-dependent ferredoxin oxidoreductase lead to impaired plant growth and restrict photosynthetic activity of transgenic tobacco plants. *Plant J* **29**: 281–293
- Harrison PW, Kruger NJ (2008) Validation of the design of feeding experiments involving [ $^{14}\text{C}$ ]substrates used to monitor metabolic flux in higher plants. *Phytochemistry* **69**: 2920–2927
- Hodges M (2002) Enzyme redundancy and the importance of 2-oxoglutarate in plant ammonium assimilation. *J Exp Bot* **53**: 905–916
- Horsch RB, Fry JE, Hoffmann NL, Eichholtz D, Rogers SG, Fraley RT (1985) A simple and general method for transferring genes into plants. *Science* **227**: 1229–1231
- Howard TP, Lloyd JC, Raines CA (2011) Inter-species variation in the oligomeric states of the higher plant Calvin cycle enzymes glyceraldehyde-3-phosphate dehydrogenase and phosphoribulokinase. *J Exp Bot* **62**: 3799–3805
- Howard TP, Metodiev M, Lloyd JC, Raines CA (2008) Thioredoxin-mediated reversible dissociation of a stromal multiprotein complex in response to changes in light availability. *Proc Natl Acad Sci USA* **105**: 4056–4061
- Hsieh MH, Lam HM, van de Loo FJ, Coruzzi G (1998) A PII-like protein in *Arabidopsis*: putative role in nitrogen sensing. *Proc Natl Acad Sci USA* **95**: 13965–13970
- Kinoshita H, Nagasaki J, Yoshikawa N, Yamamoto A, Takito S, Kawasaki M, Sugiyama T, Miyake H, Weber APM, Taniguchi M (2011) The chloroplastic 2-oxoglutarate/malate transporter has dual function as the malate valve and in carbon/nitrogen metabolism. *Plant J* **65**: 15–26
- Kopka J, Schauer N, Krueger S, Birkemeyer C, Usadel B, Bergmüller E, Dörmann P, Weckwerth W, Gibon Y, Stitt M, et al (2005) GMD@CSB. DB: the Golm Metabolome Database. *Bioinformatics* **21**: 1635–1638
- Kruger NJ, Huddleston JE, Le Lay P, Brown ND, Ratcliffe RG (2007) Network flux analysis: impact of  $^{13}\text{C}$ -substrates on metabolism in

- Arabidopsis thaliana* cell suspension cultures. *Phytochemistry* **68**: 2176–2188
- Kruger NJ, von Schaewen A** (2003) The oxidative pentose phosphate pathway: structure and organisation. *Curr Opin Plant Biol* **6**: 236–246
- Lancien M, Gadal P, Hodges M** (2000) Enzyme redundancy and the importance of 2-oxoglutarate in higher plant ammonium assimilation. *Plant Physiol* **123**: 817–824
- Lisee J, Schauer N, Kopka J, Willmitzer L, Fernie AR** (2006) Gas chromatography mass spectrometry-based metabolite profiling in plants. *Nat Protoc* **1**: 387–396
- Luedemann A, Strassburg K, Erban A, Kopka J** (2008) TagFinder for the quantitative analysis of gas chromatography-mass spectrometry (GC-MS)-based metabolite profiling experiments. *Bioinformatics* **24**: 732–737
- Maberly SC, Courcelle C, Groben R, Gontero B** (2010) Phylogenetically-based variation in the regulation of the Calvin cycle enzymes, phosphoribulokinase and glyceraldehyde-3-phosphate dehydrogenase, in algae. *J Exp Bot* **61**: 735–745
- Marri L, Trost P, Pupillo P, Sparla F** (2005) Reconstitution and properties of the recombinant glyceraldehyde-3-phosphate dehydrogenase/CP12/phosphoribulokinase supramolecular complex of *Arabidopsis*. *Plant Physiol* **139**: 1433–1443
- Marri L, Trost P, Trivelli X, Gonnelli L, Pupillo P, Sparla F** (2008) Spontaneous assembly of photosynthetic supramolecular complexes as mediated by the intrinsically unstructured protein CP12. *J Biol Chem* **283**: 1831–1838
- Marri L, Zaffagnini M, Collin V, Issakidis-Bourguet E, Lemaire SD, Pupillo P, Sparla F, Miginiac-Maslow M, Trost P** (2009) Prompt and easy activation by specific thioredoxins of Calvin cycle enzymes of *Arabidopsis thaliana* associated in the GAPDH/CP12/PRK supramolecular complex. *Mol Plant* **2**: 259–269
- Millar AH, Wiskich JT, Whelan J, Day DA** (1993) Organic acid activation of the alternative oxidase of plant mitochondria. *FEBS Lett* **329**: 259–262
- Née G, Zaffagnini M, Trost P, Issakidis-Bourguet E** (2009) Redox regulation of chloroplastic glucose-6-phosphate dehydrogenase: a new role for f-type thioredoxin. *FEBS Lett* **583**: 2827–2832
- Oesterhelt C, Klocke S, Holtgreffe S, Linke V, Weber APM, Scheibe R** (2007) Redox regulation of chloroplast enzymes in *Galdieria sulphuraria* in view of eukaryotic evolution. *Plant Cell Physiol* **48**: 1359–1373
- Paul MJ, Knight JS, Habash D, Parry MAJ, Lawlor DW, Barnes SA, Loynes A, Gray JC** (1995) Reduction in phosphoribulokinase activity by antisense RNA in transgenic tobacco: effect on CO<sub>2</sub> assimilation and growth in low irradiance. *Plant J* **7**: 535–542
- Podestá FE, Plaxton WC** (1991) Kinetic and regulatory properties of cytosolic pyruvate kinase from germinating castor oil seeds. *Biochem J* **279**: 495–501
- Pohlmeyer K, Paap BK, Soll J, Wedel N** (1996) CP12: a small nuclear-encoded chloroplast protein provides novel insights into higher-plant GAPDH evolution. *Plant Mol Biol* **32**: 969–978
- Raines CA** (2003) The Calvin cycle revisited. *Photosynth Res* **75**: 1–10
- Roessner U, Wagner C, Kopka J, Trethewey RN, Willmitzer L** (2000) Technical advance: simultaneous analysis of metabolites in potato tuber by gas chromatography-mass spectrometry. *Plant J* **23**: 131–142
- Ruuska SA, Andrews TJ, Badger MR, Price GD, von Caemmerer S** (2000) The role of chloroplast electron transport and metabolites in modulating Rubisco activity in tobacco: insights from transgenic plants with reduced amounts of cytochrome b/f complex or glyceraldehyde 3-phosphate dehydrogenase. *Plant Physiol* **122**: 491–504
- Scheibe R** (1991) Redox-modulation of chloroplast enzymes: a common principle for individual control. *Plant Physiol* **96**: 1–3
- Scheibe R** (2004) Malate valves to balance cellular energy supply. *Physiol Plant* **120**: 21–26
- Scheibe R, Backhausen JE, Emmerlich V, Holtgreffe S** (2005) Strategies to maintain redox homeostasis during photosynthesis under changing conditions. *J Exp Bot* **56**: 1481–1489
- Scheibe R, Wedel N, Vetter S, Emmerlich V, Saueremann SM** (2002) Co-existence of two regulatory NADP-glyceraldehyde 3-P dehydrogenase complexes in higher plant chloroplasts. *Eur J Biochem* **269**: 5617–5624
- Schneiderei J, Häusler RE, Fiene G, Kaiser WM, Weber APM** (2006) Antisense repression reveals a crucial role of the plastidic 2-oxoglutarate/malate translocator DiT1 at the interface between carbon and nitrogen metabolism. *Plant J* **45**: 206–224
- Singh P, Kaloudas D, Raines CA** (2008) Expression analysis of the *Arabidopsis* CP12 gene family suggests novel roles for these proteins in roots and floral tissues. *J Exp Bot* **59**: 3975–3985
- Smith CS, Weljie AM, Moorhead GBG** (2003) Molecular properties of the putative nitrogen sensor PII from *Arabidopsis thaliana*. *Plant J* **33**: 353–360
- Stitt M, Schulze D** (1994) Does Rubisco control the rate of photosynthesis and plant-growth? An exercise in molecular ecophysiology. *Plant Cell Environ* **17**: 465–487
- Tamoi M, Miyazaki T, Fukamizo T, Shigeoka S** (2005) The Calvin cycle in cyanobacteria is regulated by CP12 via the NAD(H)/NADP(H) ratio under light/dark conditions. *Plant J* **42**: 504–513
- Tompa P** (2002) Intrinsically unstructured proteins. *Trends Biochem Sci* **27**: 527–533
- Uhrig RG, Ng KKS, Moorhead GBG** (2009) PII in higher plants: a modern role for an ancient protein. *Trends Plant Sci* **14**: 505–511
- Wedel N, Soll J** (1998) Evolutionary conserved light regulation of Calvin cycle activity by NADPH-mediated reversible phosphoribulokinase/CP12/ glyceraldehyde-3-phosphate dehydrogenase complex dissociation. *Proc Natl Acad Sci USA* **95**: 9699–9704
- Wedel N, Soll J, Paap BK** (1997) CP12 provides a new mode of light regulation of Calvin cycle activity in higher plants. *Proc Natl Acad Sci USA* **94**: 10479–10484
- Wenderoth I, Scheibe R, von Schaewen A** (1997) Identification of the cysteine residues involved in redox modification of plant plastidic glucose-6-phosphate dehydrogenase. *J Biol Chem* **272**: 26985–26990
- Wingler A, Walker RP, Chen ZH, Leegood RC** (1999) Phosphoenolpyruvate carboxykinase is involved in the decarboxylation of aspartate in the bundle sheath of maize. *Plant Physiol* **120**: 539–546